John, M. J., Borjesson, B. W., Walsh, J. R., & Niall, H. D. (1981) *Endocrinology (Baltimore) 108*, 726-729.
Niall, H. D., John, M., James, R., Kwok, S., Mercado, R., Bryant-Greenwood, G., Bradshaw, R. A., Gast, M., & Boime, I. (1980) in *Insulin: Chemistry, Structure and Function of Insulin and Related Hormones* (Brandenburg, D., & Wollmer, A., Eds.) pp 719-725, de Gruyter, Berlin.
Schroeder, W. A., Shelton, J. B., & Shelton, J. R. (1969) *Arch. Biochem. Biophys. 130*, 551-556.
Schwabe, C. (1983) *Endocrinology (Baltimore) 113*, 814-815.
Schwabe, C., & Braddon, S. A. (1976) *Biochem. Biophys. Res. Commun. 68*, 1126-1132.
Schwabe, C., & McDonald, J. K. (1977) *Science (Washington, D.C.) 197*, 914-915.
Schwabe, C., McDonald, J. K., & Steinetz, B. G. (1976) *Biochem. Biophys. Res. Commun. 70*, 397-405.
Schwabe, C., McDonald, J. K., & Steinetz, B. G. (1977) *Biochem. Biophys. Res. Commun. 75*, 503-510.
Schwabe, C., Anastasi, A., Crow, H., McDonald, J. K., & Barrett, A. J. (1984) *Biochem. J. 217*, 813-817.
Sherwood, O. D. (1979) *Endocrinology (Baltimore) 104*, 886-892.
Steinetz, B. G., Beach, V. L., Kroc, R. L., Stasilli, N., Nussbaum, R., Nemith, P., & Dun, R. (1960) *Endocrinology (Philadelphia) 67*, 102-115.
Tesser, G. I., & Balvert-Geers, I. C. (1975) *Int. J. Pept. Protein Res. 7*, 295-305.
Tregear, G. W., Du, Y. C., Kemp, B., Borgesson, B. W., Scanlon, D., & Niall, H. (1981) in *Relaxin* (Bryant-Greenwood, G. D., Niall, H. D., & Greenwood, F. C., Eds.) pp 151-164, Elsevier/North-Holland, New York.
Tregear, G. W., Du, Y. C., Wang, K. Z., Southwell, C., Jones, P., John, M., Gorman, J., Kemp, B., & Niall, H. D. (1983) *Int. Congr. Ser.—Excerpta Med. No. 610*, 42-55.
Walsh, J. R., & Niall, H. D. (1980) *Endocrinology (Baltimore) 107*, 1258-1260.

Peptide Models of Electrostatic Interactions in Proteins: NMR Studies on Two β-Turn Tetrapeptides Containing Asp–His and Asp–Lys Salt Bridges†

Dinkar Sahal and P. Balaram*
Molecular Biophysics Unit, Indian Institute of Science, Bangalore 560 012, India
Received January 29, 1986; Revised Manuscript Received May 1, 1986

ABSTRACT: Two model peptides Boc-Asp-Pro-Aib-X-NHMe [X = His (**1**) and X = Lys (**2**)] were synthesized to simulate intramolecular electrostatic interactions between ionizable side chains. Conformational analysis by 270-MHz ^{1}H NMR in $(CD_3)_2SO$ reveals that the backbone secondary structures of these two peptides are stabilized by two strong intramolecular hydrogen bonds, involving the consecutive carboxy-terminal NH groups. ^{1}H NMR chemical shifts were measured in **1**, **2**, and a protected derivative, Boc-Asp(OBzl)-Pro-Aib-His-NHMe (**3**). These shifts were also measured for the model compounds Ac-Lys-NHMe, Boc-Asp-NHMe, and Boc-His-NHMe in their different states of ionization. An analysis of the chemical shifts of the ionization-sensitive reporter resonances suggests the formation of a strong intramolecular salt bridge in the lysyl peptide **2** and a bridge of moderate strength in the histidyl peptide **1**. A comparison of the temperature dependence of chemical shifts in peptides **1**–**3** suggests that intramolecular salt bridge formation results in diminished backbone flexibility. The results establish that proximity effects confer far greater stability to intramolecular ion pair interactions vis-a-vis their intermolecular counterparts. The salt bridge interaction in peptide **1** displays a remarkable sensitivity to the dielectric constant of the solvent medium. The results suggest that these peptides are good simulators of the role of salt bridges in the structural dynamics of proteins.

Electrostatic ion pair interactions in proteins influence many aspects of their behavior like thermostability, allostery, and enzyme catalysis (Perutz, 1978; Warshel, 1981; Thornton, 1982). Such interactions between amino acid side chains can play a major role in stabilizing specific secondary structures and also in mediating protein–protein interactions (Sundaralingam et al., 1985). The biochemical significance of such interactions may also be implicit in that living cells often respond to external stimuli by reversible posttranslational protein modifications like phosphorylation and methylation (Wold, 1981). These modifications alter the nature and distribution of charges on proteins, which in turn can lead to structural and functional responses.

The intrinsic sensitivity of salt bridges to pH and the fact tha fluctuations in intracellular pH provide a physiological mechanism for regulation of metabolic processes (Roos & Boron, 1981; Busa & Nuccitelli, 1984) and can also modulate intercellular communication by gating gap junctions (Spray & Bennett, 1985) emphasize the importance of these ion pair interactions in fundamental biochemical processes. pH-induced conformational changes can also play an important role in energy transduction in biological systems (Warshel, 1981). Perhaps the most remarkable role of a pH gradient is evident across a lipid bilayer in the conditions under which oxidative phosphorylation occurs (Mitchell, 1961).

While side chains of charged amino acids appear to be best suited to respond to a fluctuating pH, the general distribution of charges on the surface of proteins is often of limited con-

†Supported by a grant from the Department of Science and Technology, Government of India.
*Address correspondence to this author.

0006-2960/86/0425-6004$01.50/0

sequence. It is the microscopic interactions between ionizable groups in proteins that are features of significantly greater importance.

The undoubted importance of electrostatic ion pair interactions in modulating protein structure and function has stimulated studies on the environment of ionizable groups and their bonding patterns (Rashin & Honig, 1984) and theoretical studies of the nature and strength of interactions among charged amino acid side chains (Gilson et al., 1985; Matthew, 1985; Warshel et al., 1984; Warshel, 1981). Specific attention has been focused on the environmental sensitivity of salt bridges—a feature of considerable importance in analyzing the role of salt bridges in transmembrane peptide sequences (Honig & Hubbell, 1984). Buried charges appear to be responsible for the colors of visual pigments and bacteriorhodopsin (Nakanishi et al., 1980) and have been implicated as important elements in the photochemical energy storage mechanisms of these integral proteins (Honig et al., 1979). The problem of estimating microscopic dielectric constants in the interior of globular proteins remains a major hurdle in a reliable theoretical assessment of the contribution of ion pair interactions to protein structure and function (Warshel et al., 1984; Gilson et al., 1985).

The aim of the present investigation is to develop synthetic peptide models for a closer examination of the nature of electrostatic interactions between ionizable amino acid residues. Such peptides may be of importance in evaluating the dielectric sensitivity of salt bridges and in determining their importance in stabilizing peptide secondary structures (Mayer & Lancelot, 1981). In this paper we describe NMR studies on two synthetic model peptides, viz., Boc-Asp-Pro-Aib-X-NHMe[1] [X = His (**1**) and X = Lys (**2**)]. The Pro-Aib segment was chosen in view of its established ability to adopt β-turn conformations (Prasad & Balaram, 1984). A comparison of the Asp–His and Asp–Lys pairs in peptides **1** and **2**, respectively, should enable us to assess the relative stability of these ion pair interactions, considering the large difference in the pK values of histidine and lysine side chains. A study of peptide **1** is also of interest in view of the occurrence of the Asp-His pair in the charge-relay systems of serine and cysteine proteases (Steitz & Shulman, 1982; Polgar & Halasz, 1982) and the importance of this ion pair interaction in the alkaline Bohr effect of human hemoglobin (Perutz et al., 1985).

Experimental Procedures

Materials. Ac-Lys-NHMe and all amino acids were obtained from Sigma Chemical Co. Peptides were synthesized by conventional solution-phase procedures, which are briefly described below. Intermediate peptides were carried through without extensive purification. ^{1}H NMR spectroscopy (60/80/270 MHz) was routinely used for establishing the identity of the intermediates. All final peptides were purified by silica gel column chromatography with $CH_3OH/CHCl_3$ elution systems. Purity of these peptides was checked by thin-layer chromatography (TLC) in various solvent systems [chloroform–methanol (9:1, v/v) (A); chloroform–methanol–acetic acid (85:10:5, v/v) (B); butanol–acetic acid–water (4:1:1, v/v) (C)] and confirmed by high-performance liquid chromatography (HPLC) on a Lichrosorb RP-18 column with linear gradients of methanol in water. Peptides **1**–**3** were also characterized by 270-MHz ^{1}H NMR spectroscopy and amino acid analyses.

Boc-Pro-Aib-His-OMe. His-OMe·2HCl (9.68 g, 40 mmol) was suspended in dry $CHCl_3$ and cooled to 0 °C. Dry ammonia was bubbled for ~20 min. NH_4Cl was filtered out, and the filtrate was evaporated to yield His-OMe as a gum (7 g, 40 mmol), which was dissolved in 10 mL of DMF. Boc-Pro-Aib-OH (Balasubramanian et al., 1981) (12 g, 40 mmol) and HOBt (6.8 g, 45 mmol) were dissolved in stirring DMF (50 mL, 0 °C), and dicyclohexylcarbodiimide (DCC) (8.2 g, 40 mmol) was added. After 4 min, the His-OMe solution was added to the reaction mixture. Stirring was continued overnight. Dicyclohexylurea (DCU) was filtered off and DMF evaporated in vacuo. The residue was taken in EtOAc and washed with 10% Na_2CO_3 solution and saline, respectively, and finally dried over Na_2SO_4. Evaporation yielded the tripeptide as a white solid [6 g, 33%; R_f 0.4 (A)].

Boc-Pro-Aib-His-NHMe. Boc-Pro-Aib-His-OMe (5 g, 11 mmol) was dissolved in methanol, and dry methylamine gas was bubbled till saturation. The flask was tightly stoppered and kept overnight at room temperature. Evaporation of the solvent gave the tripeptide as a gum [4.7 g, 94%, R_f 0.26 (A)].

Pro-Aib-His-NHMe. Boc-Pro-Aib-His-NHMe (1.8 g, 4 mmol) was treated with HCl in dry THF containing 5% (v/v) anisole for 30 min, at the end of which TLC showed complete removal of the Boc group. Solvent was evaporated, and the residue obtained was suspended in dry chloroform (0 °C) and ammonia gas bubbled for ~20 min. The precipitated NH_4Cl was filtered and the filtrate evaporated in vacuo to give the tripeptide-free base as a gum (1.2 g, 85%).

Boc-Asp(OBzl)-Pro-Aib-His-NHMe (**3**). To a stirred solution of Boc-Asp(OBzl) (1.13 g, 3.5 mmol) and HOBt (0.61 g, 4 mmol) in DMF (8 mL, 0 °C) DCC (0.77 g, 3.75 mmol) was added. After a lapse of 4 min, a solution of Pro-Aib-His-NHMe (1.2 g, 3.4 mmol) in 2 mL of DMF was added to the reaction mixture. Stirring was continued overnight at room temperature. DCU was filtered off and DMF evaporated in vacuo. The residue was taken in EtOAc and washed with 10% Na_2CO_3 and brine, respectively, and finally dried over Na_2SO_4. Evaporation yielded a gum (1.6 g), which was further purified by silica gel column chromatography. The peptide eluting at 3% $CH_3OH/CHCl_3$ was obtained as a white solid, which was Pauly positive (Stewart & Young, 1969) and showed the characteristic ultraviolet spectrum of the benzyl chromophore. ^{13}C (67.89-MHz) and ^{1}H (270-MHz) NMR spectra were fully consistent with its structure (yield 590 mg, 26%, mp 110 °C). Amino acid analysis gave the following: Asp, 1.0 (1); Pro, 1.0 (1); His, 0.90 (1). Aib was not estimated due to its low ninhydrin color value.

Boc-Asp-Pro-Aib-His-NHMe (**1**). Boc-Asp(OBzl)-Pro-Aib-His-NHMe (180 mg, 0.27 mmol) was dissolved in 10 mL of CH_3OH–H_2O (9:1) and mixed with 20 mg of palladium black. Hydrogen gas was bubbled till TLC showed hydrogenolysis to be complete [R_f 0.1 (A)]. The catalyst was filtered off and the filtrate evaporated in vacuo to obtain a gum. This was taken in water and washed with EtOAc. Lyophilization of the aqueous layer gave a white, fluffy, hygroscopic solid [R_f 0.1 (A), 0.5 (C)]. The peptide showed a ^{1}H NMR spectrum (270 MHz) fully consistent with its structure (Figure 1). The peptide gave a satisfactory amino acid analysis: Asp, 1.2 (1.0); Pro, 1.0 (1.0); His, 0.86 (1.0). Aib was not estimated due to its poor ninhydrin color value.

[1] Abbreviations: Ac, acetyl; Aib, α-aminoisobutyric acid; Boc, *tert*-butyloxycarbonyl; $(CD_3)_2SO$, dimethyl-d_6 sulfoxide; $CDCl_3$, chloroform-d; DCC, dicyclohexylcarbodiimide; DCU, dicyclohexylurea; DSS, sodium salt of 2,2-dimethyl-2-silapentane-5-sulfonate; DMF, dimethylformamide; HOBt, hydroxybenzotriazole; EtOAc, ethyl acetate; HPLC, high-performance liquid chromatography; mp, melting point; min, minute(s); NHMe, methylamide; THF, tetrahydrofuran; TMS, tetramethylsilane; TLC, thin-layer chromatography; Z, benzyloxycarbonyl.

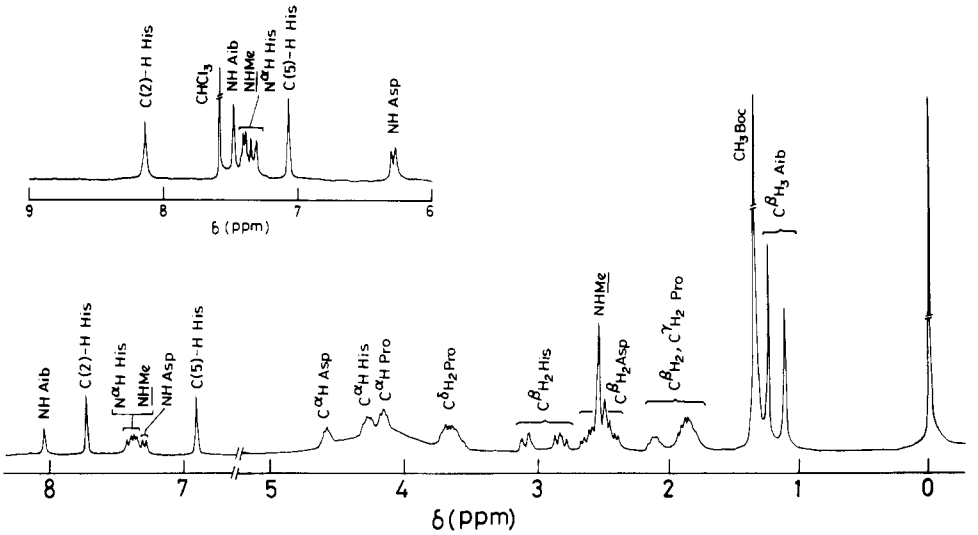

FIGURE 1: The 270-MHz ^1H NMR spectrum of Boc-Asp-Pro-Aib-His-NHMe (**1**) (12 mM) in $(CD_3)_2SO$. (Inset) Peptide NH resonances in a $(CD_3)_2SO$–$CDCl_3$ mixture (1:3).

Boc-Pro-Aib-Lys(Z)-NHMe. Boc-Pro-Aib-Lys(Z)-OMe (gum, yield 60%) and Boc-Pro-Aib-Lys(Z)NHMe (gum) were synthesized from Boc-Pro-Aib-OH and Lys(Z)-OMe by using essentially the same procedures as described for the corresponding histidyl peptides.

Boc-Asp(OBzl)-Pro-Aib-Lys(Z)-NHMe. Boc-Asp(OBzl) (0.581 g, 1.8 mmol) and Pro-Aib-Lys(Z)-NHMe [0.870 g, 1.8 mmol; obtained by treating Boc-Pro-Aib-Lys(Z)-NHMe with HCl–THF for 30 min and extracting the peptide into chloroform from an aqueous solution of pH 10] were dissolved while being stirred in DMF (5 mL, 0 °C). HOBt (0.306 g, 2 mmol) was added, followed by addition of DCC (0.371 g, 1.8 mmol). Stirring was continued overnight. DCU was filtered off and the reaction worked up by successive washings with 10% citric acid, 10% Na_2CO_3, and brine. Evaporation of the organic layer gave a hygroscopic, yellowish solid (1.1 g). This was further purified on a silica gel column. The peptide eluting at 1% $CH_3OH/CHCl_3$ gave a white, hygroscopic solid on evaporation [300 mg, 21%; R_f 0.7 (A)]. The purity of the product was confirmed by HPLC with a Lichrosorb RP-18 column (linear gradient 60–95% CH_3OH–H_2O in 30 min, flow 0.8 ml min^{-1}; detector 226 nm; retention time 16.6 min).

Boc-Asp-Pro-Aib-Lys-NHMe (**2**). Catalytic transfer hydrogenolysis (Anwer & Spatola, 1980) was done on Boc-Asp(OBzl)-Pro-Aib-Lys(Z)-NHMe (300 mg) by dissolving it in 10 mL of CH_3OH–H_2O (9:1) containing 30 mg of paladium black. A total of 100 mg ammonium formate was added and the reaction kept stirring overnight. The catalyst was filtered out and solvent evaporated in vacuo. The residue was taken in water and washed four times with EtOAc. The aqueous layer was lyophilized to yield a white, hygroscopic solid (303 mg). The peptide was purified by passing it through a Sephadex G-10 column (26 cm × 2 cm). The ninhydrin-positive material, which was not overlapping with the excess ammonium formate peak, was pooled and lyophilized to give a white, hygroscopic solid (260 mg). The peptide gave a 270-MHz ^1H NMR spectrum fully consistent with its structure (Figure 2). Its composition was verified by a satisfactory amino acid analysis: Asp, 0.93 (1); Pro, 1.05 (1); Lys, 1.0 (1). The Aib value was not obtained due to the low color value of its ninhydrin reaction.

NMR Studies. The ^1H (270-MHz) NMR spectra were recorded on a WH 270 Bruker spectrometer at the Sophisticated Instruments Facility, Indian Institute of Science, Bangalore. A convolution difference routine was used to enhance spectral resolution in specific cases. All ^1H chemical shifts in organic solvents are expressed as ppm downfield of tetramethylsilane (TMS), while shifts in water are with respect to the sodium salt of 2,2-dimethyl-2-silapentane-5-sulfonate (DSS). NMR analyses of hydrogen-bonded NH groups were carried out as described earlier (Nagaraj & Balaram, 1981a).

RESULTS

NMR Studies. Figures 1 and 2 show the 270-MHz ^1H NMR spectra of Boc-Asp-Pro-Aib-His-NHMe (**1**) and Boc-Asp-Pro-Aib-Lys-NHMe (**2**), respectively, in $(CD_3)_2SO$. Inset b in Figure 2 and the inset in Figure 1 show the amide NH regions of these peptides in a mixture of $CDCl_3$ and $(CD_3)_2SO$.

The Asp NH resonance in both peptides **1** and **2** was easily recognized by virtue of its appearance at a relatively high-field (δ = 6.3–6.5 ppm) position in a mixture of $CDCl_3$ and $(CD_3)_2SO$ (Bystrov et al., 1969; Nagaraj & Balaram, 1981a; Iqbal & Balaram, 1981) and by its tendency to show exchange broadening with increasing temperature in $(CD_3)_2SO$. This is a feature commonly observed for the urethane NH protons (Iqbal & Balaram, 1981). A broad resonance is observed in the low-field region for peptide **2**, arising from the labile side-chain protons that are exchanging with water present in the solvent. As shown in Figure 2 (inset a), this broad resonance was abolished on irradiation of the water signal at δ = 3.5 ppm, the suppression arising from transfer of saturation from protons of water via chemical-exchange processes. This broad signal disappears also at high temperatures (~311 K) when the exchange rate is enhanced.

Homonuclear decoupling of the $C^{\alpha}H$ resonances was used to identify the corresponding $N^{\alpha}H$ and $C^{\beta}H_2$ connectivities. The methylamide NH group was identified as the only quartet resonance. The singlet resonance exchangeable with D_2O was assigned to the Aib NH group. The remaining doublet NH resonance was assigned to His/Lys $N^{\alpha}H$ groups in the corresponding peptides. The spectrum of peptide **2** (X = Lys) Figure 2) showed a singlet resonance at 8.2 ppm, which did not exchange with D_2O. This was assigned to the formate proton resonance arising from traces of ammonium formate in the peptide. Indeed, repeated lyophilizations of the sample caused progressive decrease in the intensity of this resonance. The two sharp singlets in the spectrum of peptide **1** (X = His) (Figure 1) that did not exchange with D_2O were assigned to the C(2)–H (7.75 ppm) and the C(5)–H^2 (6.92 ppm) ring

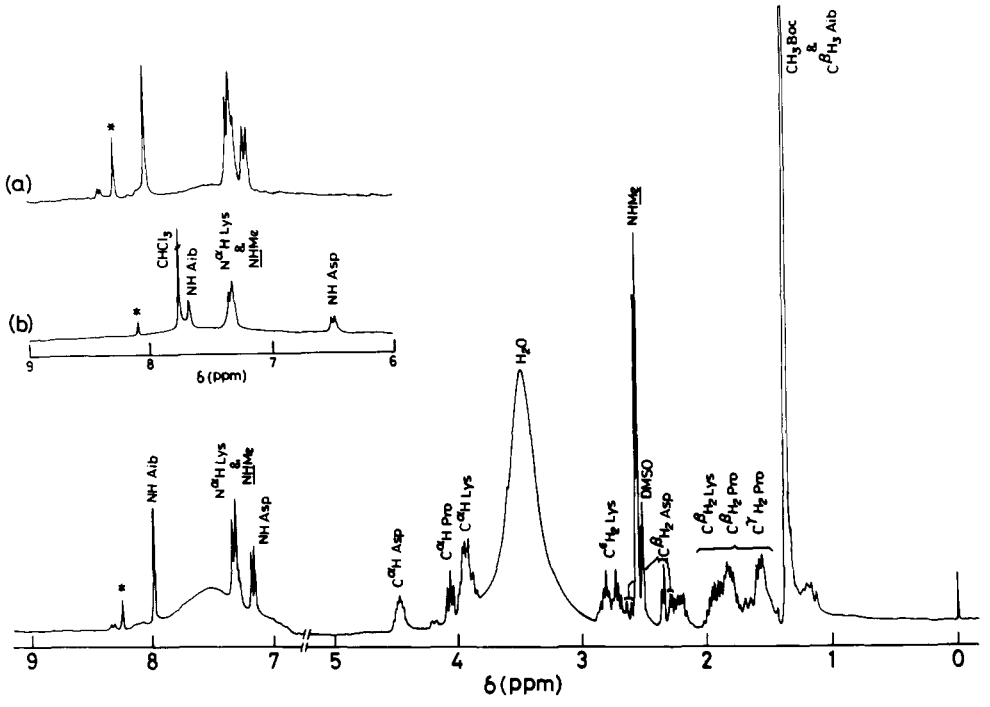

FIGURE 2: The 270-MHz ^1H NMR spectrum of Boc-Asp-Pro-Aib-Lys-NHMe (**2**) (12 mM) in $(CD_3)_2SO$. Peaks marked with an asterisk (*) indicate residual formate protons. (Inset a) H_2O resonance at ~3.5 ppm has been irradiated. Note the disappearance of the broad resonance at ~7.5 ppm. (Inset b) Peptide NH resonances in a $(CD_3)_2SO$–$CDCl_3$ mixture (1:3).

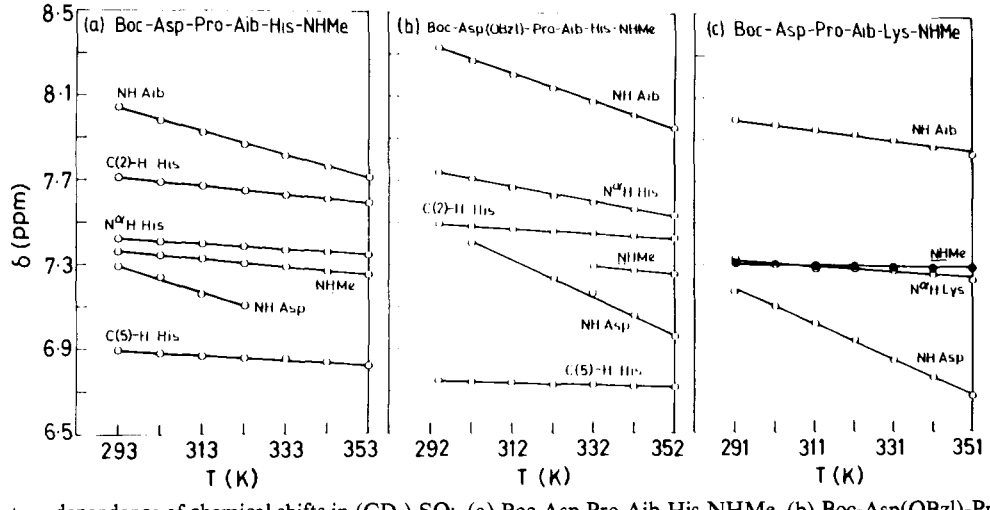

FIGURE 3: Temperature dependence of chemical shifts in $(CD_3)_2SO$: (a) Boc-Asp-Pro-Aib-His-NHMe, (b) Boc-Asp(OBzl)-Pro-Aib-His-NHMe, and (c) Boc-Asp-Pro-Aib-Lys-NHMe. The peptide concentrations are ~12 mM each.

Table I: ^1H NMR Backbone Parameters for Peptides **1**–**3**[a]

	Boc-Asp-Pro-Aib-His-NHMe					Boc-Asp-Pro-Aib-Lys-NHMe				
parameters	Asp	Pro	Aib	His	NHMe	Asp	Pro	Aib	Lys	NHMe
$\delta_{NH}[(CD_3)_2SO]$	7.29 (7.45)[d]		8.04 (8.30)	7.43 (7.75)	7.37 (7.35)	7.17		7.99	7.33	7.31
$\delta_{NH}[CDCl_3 + (CD_3)_2SO]$[b]	6.49		7.66	7.33	7.33	6.52		7.68	7.35	7.33
$\delta_{C^\alpha H}[(CD_3)_2SO]$	4.58 (4.25)	4.16 (4.25)		4.28 (4.63)		4.48	4.05		3.95	
$d\delta/dT$[c]	0.0067 (0.0082)		0.0054 (0.0064)	0.0013 (0.0035)	0.0019 (0.0020)	0.0083		0.0027	0.0017	0.0004

[a] Peptide concentration is 12 mM. [b] The mixture is 25% $(CD_3)_2SO$ in $CDCl_3$. [c] $d\delta/dT$ values are determined in $(CD_3)_2SO$ and expressed as ppm/K. [d] Figures in parentheses represent values obtained for Boc-Asp(OBzl)-Pro-Aib-His-NHMe (**3**).

protons of histidine (Roberts & Jardetzky, 1970; Markley, 1975). Assignments in Boc-Asp(OBzl)-Pro-Aib-His-NHMe (**3**) were made in analogous fashion. Table I shows the ^1H NMR backbone parameters for peptides **1**–**3**.

Backbone Conformations of Tetrapeptides. (*A*) *Boc-Asp-Pro-Aib-His-NHMe* (**1**). Figure 3a establishes a linear temperature dependence of chemical shifts in $(CD_3)_2SO$ for the peptide NH resonances and for the C(2)–H and C(5)–H resonances of the imidazole group. The temperature coefficients ($d\delta/dT$) are listed in Table I. It may be noted that there was no perceptible concentration dependence of chemical shifts

[2] Note that the numbering adopted for the imidazole ring of histidine follows recommendations of the IUPAC–IUB Commission on Biochemical Nomenclature (1984). The C(5)–H referred to in this paper has often been designated as C(4)–H in the literature.

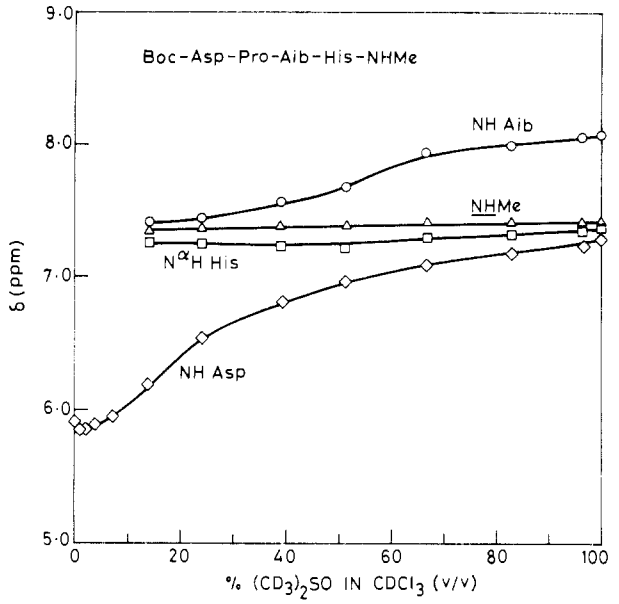

FIGURE 4: Chemical shifts of peptide backbone NH groups in Boc-Asp-Pro-Aib-His-NHMe (**1**) as a function of varying concentrations of $(CD_3)_2SO$ in $CDCl_3$. Peptide concentration is ~12 mM.

in $(CD_3)_2SO$ in the peptide concentration range of 4–40 mM, suggesting the absence of effects due to intermolecular peptide aggregation.

Solvent-exposed NH protons typically have $d\delta/dT$ values >0.004 ppm/K, while solvent-shielded protons have $d\delta/dT$ values <0.003 ppm/K (Hruby, 1974). The results in Table I indicate that the His N$^{\alpha}$H and the methylamide NH groups are strongly solvent shielded, presumably due to their involvement in strong intramolecular hydrogen bonds. The Asp NH group is clearly exposed to the solvent. The Aib NH group has a $d\delta/dT$ value characteristic of a solvent-exposed NH (see Discussion). The solvent dependence of chemical shifts in $CDCl_3$–$(CD_3)_2SO$ mixtures is shown in Figure 4. The Asp NH group shows a large downfield chemical shift on addition of $(CD_3)_2SO$, a hydrogen-bonding solvent. A smaller shift is observed for the Aib NH group. The methylamide NH and His N$^{\alpha}$H groups are inaccessible to the solvent and exhibit negligible solvent dependence of chemical shifts. These results provide further support for the conclusion that the Asp NH group is free and solvent-exposed, while the His N$^{\alpha}$H and methylamide NH groups are strongly solvent shielded presumably due to formation of strong intramolecular hydrogen bonds.

(*B*) *Boc-Asp(OBzl)-Pro-Aib-His-NHMe* (**3**). Figure 3b shows the temperature dependence of chemical shifts for the backbone NH resonances and the C(2)–H and C(5)–H (His imidazole ring) resonances. A linear dependence is observed. The temperature coefficients ($d\delta/dT$), listed in Table I, suggest the solvent-exposed nature of the Asp and Aib NH groups and the solvent-shielded, presumably hydrogen-bonded nature of His N$^{\alpha}$H and methylamide NH groups. It is notable that the observed $d\delta/dT$ values are higher in this peptide than in **1**, which has a free aspartyl carboxyl group.

(*C*) *Boc-Asp-Pro-Aib-Lys-NHMe* (**2**). The peptide showed no concentration dependence of chemical shifts in $(CD_3)_2SO$ in the range 12–40 mM, suggesting negligible interpeptide interactions under these conditions. Figure 3c establishes a linear temperature dependence of the NH chemical shifts in $(CD_3)_2SO$. The temperature coefficients ($d\delta/dT$) listed in Table I clearly suggest that the Asp NH group is freely solvent exposed, while the two consecutive carboxy-terminal NH groups, viz., Lys N$^{\alpha}$H and methylamide NH groups, are

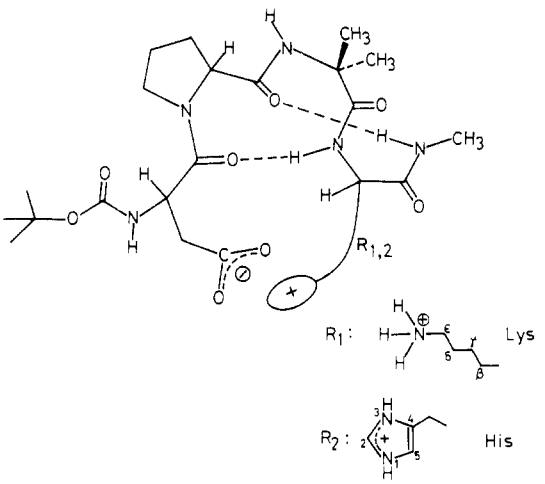

FIGURE 5: Schematic representation of solution conformation of Boc-Asp-Pro-Aib-His-NHMe (**1**) and Boc-Asp-Pro-Aib-Lys-NHMe (**2**) as deduced from 270-MHz ^1H NMR studies.

solvent shileded and presumably strongly intramolecularly hydrogen bonded. It is interesting to note that the $d\delta/dT$ value for the methylamide NH group is much lower for this peptide than in the case of the histidyl analogue **1**. The Aib NH group appears to be partially solvent shielded.

Conformation of Tetrapeptides. The presence of a -Pro-Aib- segment in these tetrapeptides should facilitate formation of β-turn conformations (Prasad & Balaram, 1983, 1984), with Pro and Aib at the $i + 1$ and $i + 2$ positions, respectively. Considerable evidence for the ability of Pro-Aib segments to form type II ($\phi_{Pro} = -60°$, $\psi_{Pro} = 120°$, $\phi_{Aib} = 80°$, $\psi_{Aib} = 0°$) or type III ($\phi_{Pro} = -60°$, $\psi_{Pro} = -30°$, $\phi_{Aib} = -60°$, $\psi_{Aib} = -30°$) β-turns exists in the literature; e.g., Piv–Pro-Aib-NHMe has been shown to adopt a type II β-bend (Prasad et al., 1982) whereas the cyclic peptide Boc-Cys-Pro-Aib-Cys-NHMe adopts a type III β-bend in solution (Ravi et al., 1983). Furthermore, Aib-X sequences also show a strong tendency to form β-turns (Prasad & Balaram, 1984; Nagaraj & Balaram, 1981b). The NMR evidence strongly suggests that both carboxy-terminal NH groups (His/Lys N$^{\alpha}$H and NHMe) in peptides **1**–**3** are solvent-shielded. The data are thus consistent with peptide conformations in which both these NH groups are intramolecularly hydrogen bonded.

Consecutive β-turn structures involving type III-III conformations (incipient 3_{10} helix, $\phi_{Pro} = \phi_{Aib} = \phi_X = -60°$, $\psi_{Pro} = \psi_{Aib} = \psi_X = -30°$) or type II-III′ conformations ($\phi_{Pro} = -60°$, $\psi_{Pro} = 120°$, $\phi_{Aib} = 70°$, $\psi_{Aib} = 20°$, $\phi_X = 70°$, $\psi_X = 20°$) for the Pro-Aib-X segment (Ravi & Balaram, 1984) indeed result in the hydrogen-bonding scheme deduced from NMR. In both structures, two intramolecular 4→1 hydrogen bonds (Asp CO---N$^{\alpha}$H Lys/His; Pro CO---NHMe) are possible (Figure 5). It may be noted that β-turn conformations of both types have been observed in peptides with Pro-Aib-X segments. For example, a consecutive type III-III conformation has been observed in the crystal structure of Boc-Pro-Aib-Ala-Aib-OBzl (Smith et al., 1981), while a type II-III′ structure is observed for *p*-chlorobenzoyl-Pro-Aib-Ala-Aib-Ala-OMe in the solid state (Cameron et al., 1982).

Peptides **1** and **2** probably adopt fairly rigid consecutive β-turn backbone conformations in solution. In such structures, there is a good likelihood of close proximal interactions between the ionizable side chains (Figure 5).

State of Ionization of Side Chains in Peptides **1** *and* **2**. Chemical shifts of the C(2)–H His, C$^{\epsilon}$H$_2$ Lys, and C$^{\beta}$H$_2$ Asp protons are diagnostic of the state of ionization of these residues. Protonation of the imidazole group of histidine or the

Table II: Diagnostic Chemical Shifts (ppm)[a] in His, Lys, and Asp Derivatives and Peptides (**1**–**3**)

resonance	Ac-Lys-NHMe	[Ac-Lys-NHMe]$^+$-CD_3COO^-	Ac-Lys-NHMe + Boc-Asp-NHMe[b]	Boc-Asp-Pro-Aib-Lys-NHMe	Boc-Asp-NHMe	[Boc-Asp-NHMe]$^-$Na$^+$
$C^\epsilon H_2$ (Lys)	2.49	2.70	2.70	2.81, 2.73		
$C^\beta H_2$ (Asp)			2.34	2.32, 2.60	2.60, 2.42	2.28, 2.15

resonance	Boc-His-NHMe	[Boc-His-NHMe]$^+$-CD_3COO^-	Boc-His-NHMe + Boc-Asp-NHMe	Boc-Asp(OBzl)-Pro-Aib-His-NHMe	Boc-Asp-Pro-Aib-His-NHMe
His C(2)–H	7.54 (7.53)[c]	7.58 (8.05)	7.56 (8.19)	7.49 (7.51)	7.71 (8.34)
His C(5)–H	6.74 (6.80)	6.81 (6.95)	6.75 (6.99)	6.75 (6.75)	6.89 (7.12)
Asp $C^\beta H_2$			2.58, 2.39	2.58, 2.76	2.65, 2.45

[a] Chemical shifts (δ, ppm) have been measured in $(CD_3)_2SO$ at concentrations of ~12 mM. [b] An equimolar mixture (12 mM) of the two derivatives has been taken. [c] Figures in parentheses represent chemical shifts observed in $CDCl_3$.

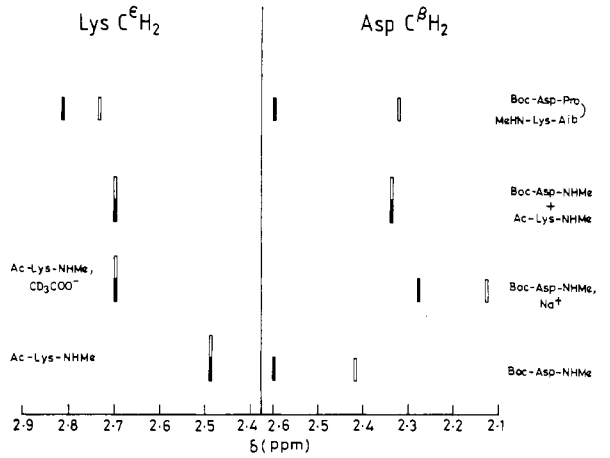

FIGURE 6: Schematic representation of ionization reporter chemical shifts, viz., $C^\beta H_2$ (Asp) and $C^\epsilon H_2$ (Lys), observed in the indicated model compounds and in peptide **2**. All compounds were studied at a concentration of ~12 mM in $(CD_3)_2SO$. Shaded and open bars represent the two diastereotopic protons of the methylene groups.

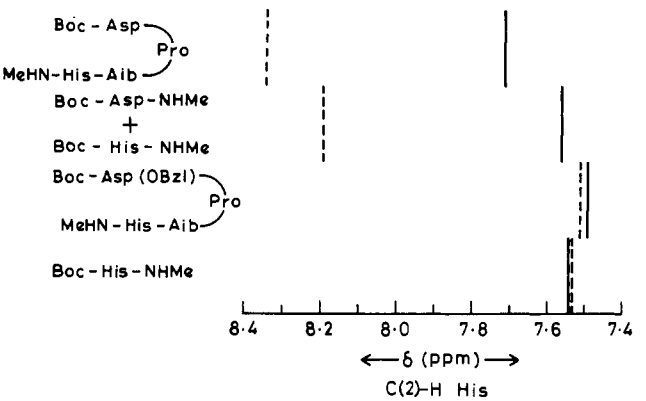

FIGURE 7: Chemical shifts of His C(2)–H in Boc-His-NHMe, Boc-Asp(OBzl)-Pro-Aib-His-NHMe, Boc-Asp-NHMe + Boc-His-NHMe, and Boc-Asp-Pro-Aib-His-NHMe recorded in $(CD_3)_2SO$ (—) and in $CDCl_3$ (– –). Peptide/amino acid derivatives concentration is ~12 mM.

ϵ-amino group of the lysine side chain leads to down-field shifts of the C(2)–H His (~1 ppm), C(5)–H His (~0.4 ppm), or $C^\epsilon H_2$ Lys (~0.5 ppm) protons in the case of the free amino acids in aqueous solutions. In the case of aspartic acid, deprotonation results in an upfield shift of the $C^\beta H_2$ protons (~0.3 ppm) (Roberts & Jardetzky, 1970). These reporter shifts for side chains of ionizable amino acids in different states of ionization have been generally determined in aqueous solutions, and there are limited data for these chemical shifts in organic solvents. Therefore, in this study, the ionization reporter chemical shifts in Boc-His-NHMe, Boc-Asp-NHMe, and Ac-Lys-NHMe and their equimolar mixtures have been measured in $CDCl_3$ and/or $(CD_3)_2SO$.

Ac-Lys-NHMe and Boc-His-NHMe were converted to their acetate salts by lyophilization from acetic acid solutions. Boc-Asp-NHMe was converted to its sodium salt by lyophilization from an aqueous solution of sodium hydroxide. The histidine peptides (**1** and **3**) and derivatives were studied in $CDCl_3$ and $(CD_3)_2SO$, while the lysine peptide **2** and derivatives could be studied only in $(CD_3)_2SO$ or mixtures of $(CD_3)_2SO$ and $CDCl_3$ for reasons of solubility.

The chemical shifts of the relevant side chains in various peptides and derivatives are listed in Table II. Figures 6 and 7 summarize schematically the observed chemical shifts in the lysine and histidine series, respectively.

Lysine–Aspartic Acid Side-Chain Interactions. The $C^\epsilon H_2$ protons of Lys in Ac-Lys-NHMe appear as a triplet at 2.49 ppm in $(CD_3)_2SO$. Protonation of the ϵ-NH_2 groups leads to a downfield shift of the $C^\epsilon H_2$ resonance, which is observed at 2.70 ppm in acetate. Addition of an equimolar amount of Boc-Asp-NHMe to Ac-Lys-NHMe also results in precisely the same downfield chemical shift (2.70 ppm), suggesting proton transfer from the aspartyl side chain to the lysyl side chain. In peptide **2**, the $C^\epsilon H_2$ protons of lysine appear at 2.82 and 2.75 ppm, respectively, providing firm evidence for the protonated state of the ϵ-NH_2 group. The geminal $C^\epsilon H_2$ protons in **2** appear as distinct multiplets, exhibiting their magnetic nonequivalence (Figures 2 and 6). In principle, the $C^\epsilon H_2$ protons are diastereotopic in all lysine derivatives and may be expected to be chemical shift nonequivalent. However, the two protons invariably appear as a triplet resonance in simple lysine derivatives, suggesting that chemical shift differences, if any, between the two protons are very small in these cases. The enhanced chemical shift nonequivalence in **2** may be a consequence of the decreased mobility of the lysine side chain owing to its participation in an intramolecular salt bridge. Indeed, the requirements of multiple hydrogen-bonding interactions in an ideal salt bridge impose considerable geometrical restraints and should, in principle, result in a population of specific rotamers about the C–C bonds of the tetramethylene side chain in lysine.

The magnitude of the chemical shift difference between the $C^\epsilon H_2$ protons diminishes only marginally at elevated temperatures and is not abrogated even at the highest temperature of this study. Thus, these values for $C^\epsilon H_2$ are 2.81 and 2.73 ppm at 291 K and 2.78 and 2.74 ppm at 351 K. The distinct multiplet pattern of the individual $C^\epsilon H_2$ protons is maintained through the entire temperature range of 291–351 K. These observations reflect a significant stability of the salt bridge interaction, even at elevated temperatures. A contrast is presented by the equimolar mixture of Boc-Asp-NHMe and Ac-Lys-NHMe (Figure 6). Here, while the $C^\epsilon H_2$ protons exhibit chemical shifts indicating formation of an ammonium ion, the resonance appears as a mere triplet, which broadens

with increasing temperature. This line broadening may be a consequence of the temperature-dependent exchange between moderately tight ion pairs and fully solvated ionic species.

The $C^{\beta}H_2$ protons of aspartic acid are nonequivalent in the derivative Boc-Asp-NHMe and appear at 2.60 and 2.42 ppm as the eight-line AB subspectrum of an ABX spin system. Deprotonation of the carboxyl group in [Boc-Asp-NHMe]$^-$ Na^+ results in an upfield shift (2.28 and 2.15 ppm) of both of the $C^{\beta}H_2$ protons (Table II; Figure 6). In the equimolar mixture of Boc-Asp-NHMe and Ac-Lys-NHMe, the $C^{\beta}H_2$ (Asp) protons appear as a doublet resonance at 2.34 ppm. This is due to accidental chemical shift equivalence of the two diastereotopic protons.

Chemical shifts of 2.32 and 2.60 ppm, respectively, are observed for the $C^{\beta}H_2$ (Asp) protons in peptide **2**. This large geminal nonequivalence is likely to be a consequence of the population of specific rotamer species about the C^{α}–C^{β} and the C^{β}–COO^- bonds, leading to enhanced magnetic nonequivalence of the $C^{\beta}H_2$ protons, with an anomalously low-field chemical shift of one of the two protons. Such shielding effects can easily result from preferential orientation of the magnetically anisotropic carboxylate group. This, in turn, may arise from involvement of the carboxylate group in a specific interaction with the ammonium ion of lysine, which may impose considerable geometrical restraints.

Some evidence for altered rotamer population is obtained also from the observed $J_{C^{\alpha}H_X-C^{\beta}H_{A,B}}$ values. These are 2.9 and 6.6 Hz ([Boc-Asp-NHMe]$^-$$Na^+$), 5.4 and 8.5 Hz (Boc-Asp-NHMe), and 5.4 and 10.8 Hz (Boc-Asp-Pro-Aib-Lys-NHMe).

Histidine–Aspartic Acid Side-Chain Interactions. The chemical shifts of the Asp $C^{\beta}H_2$, His C(2)–H, and His C(5)–H protons in the amino acid derivatives in different states of ionization and for peptides **1** and **3** are presented in Table II. The chemical shifts of His C(2)–H in Boc-His-NHMe, an equimolar mixture of Boc-His-NHMe and Boc-Asp-NHMe, and peptides **1** and **3** are schematically shown in Figure 7. In the protected peptide **3** and in the neutral derivative Boc-His-NHMe, the C(2)–H proton appears at a relatively high-field position (~7.5 ppm) in both $CDCl_3$ and $(CD_3)_2SO$. This chemical shift is characteristic of an uncharged imidazole. Protonation of the imidazole results in a downfield shift of the C(2)–H resonance. This is evident on addition of an equimolar amount of Boc-Asp-NHMe to Boc-His-NHMe in $CDCl_3$, where a C(2)–H chemical shift of 8.19 ppm is observed. In peptide **1**, the C(2)–H signal appears at an extremely low-field position (8.34 ppm) in $CDCl_3$, strongly suggesting that the imidazole ring in **1** is protonated under these conditions.

It is of particular interest to note that in both peptide **1** and the equimolar mixture of Boc-Asp-NHMe and Boc-His-NHMe the C(2)–H protons resonate at relatively high fields when they are solvated in $(CD_3)_2SO$. This effect is pronounced for the equimolar mixture of Boc-Asp-NHMe and Boc-His-NHMe, where the C(2)–H chemical shift of 7.56 ppm would suggest a fully neutral imidazole species. Interestingly enough, though the C(2)–H signal in **1** shows a considerable shift on going from $CDCl_3$ to $(CD_3)_2SO$, the $(CD_3)_2SO$ value of 7.71 ppm is still ~0.2 ppm downfield with respect to a neutral imidazole.

These observations suggest an important role of solvent and proximity effects in determining the state of ionization of histidine and aspartic acid in these systems. In order to examine these features in greater detail, C(2)–H chemical shifts for **1** and equimolar mixtures of Boc-Asp-NHMe and Boc-His-NHMe were determined in mixtures of $CDCl_3$ and

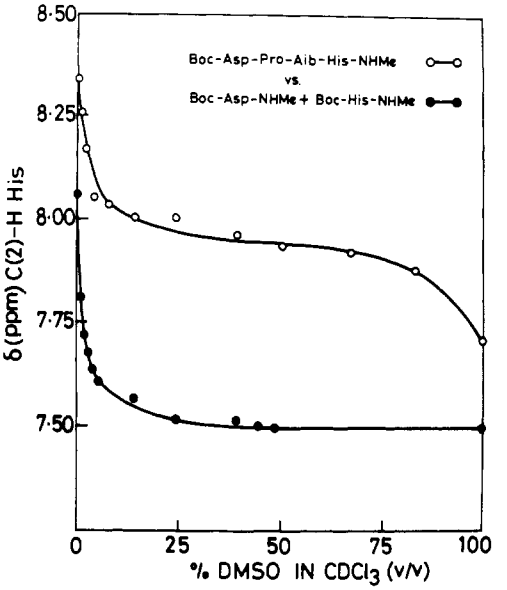

FIGURE 8: Chemical shifts of the His C(2)–H proton as a function of varying concentration of $(CD_3)_2SO$ in $CDCl_3$: (○) Boc-Asp-Pro-Aib-His-NHMe (12.4 mM); (●) Boc-Asp-NHMe (12.4 mM) + Boc-His-NHMe (12.4 mM).

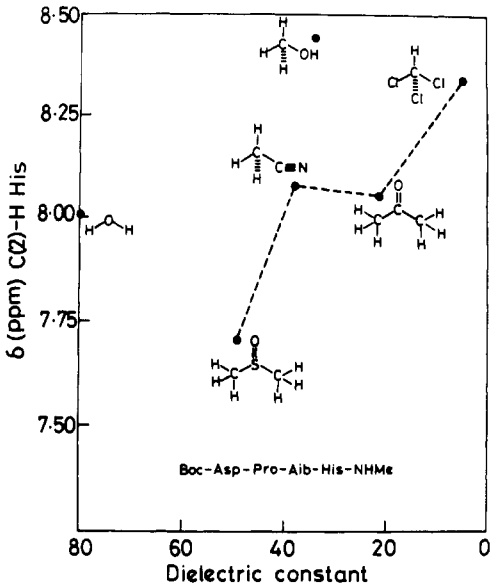

FIGURE 9: Chemical shifts for His C(2)–H proton in Boc-Asp-Pro-Aib-His-NHMe (**1**) (10 mM) measured in the indicated solvents and plotted against the solvent dielectric constant. Internal standard used was DSS for D_2O and TMS for all other solvents.

$(CD_3)_2SO$. These results are shown in Figure 8. In both cases, there is a pronounced upfield chemical shift of the His C(2)–H resonance on addition of $(CD_3)_2SO$ up to a concentration of 15% (v/v). The observed upfield shift is more significant for the mixture of Boc-Asp-NHMe and Boc-His-NHMe than for peptide **1**. Furthermore, the His C(2)–H resonance in the peptide appears at distinctly lower fields over the entire range of solvent composition, as compared to the shifts seen for the mixture of derivatives. These results suggest that the intramolecular interaction between aspartyl and histidyl side chains as modeled in **1** is appreciably stronger than the intermolecular interaction observed in the mixture of Boc-Asp-NHMe and Boc-His-NHMe.

In order to further characterize the solvent sensitivity of interaction between the ionized side chains of peptide **1**, chemical shifts of the His C(2)–H protons were measured in several different solvents. Figure 9 shows a plot of these

chemical shifts vs. dielectric constants (ϵ) of the solvents. If the four aprotic solvents dimethyl sulfoxide, acetone, acetonitrile, and chloroform are considered, there appears to be an enhanced downfield shift of the His C(2)–H proton on lowering of the dielectric constant. A plateau is observed in the region of $\epsilon \sim 20$–40. It is of interest to note that such a plateau also appears in the plot (Figure 8) depicting C(2)–H chemical shifts in **1** as a function of increasing concentration of $(CD_3)_2SO$ in $CDCl_3$. The protic solvents water and methanol show anomalously low-field shifts. The chemical shift of 8.4 ppm observed in methanol is characteristic of a completely protonated imidazole. The value of 8.0 ppm observed in neutral water would also argue for appreciable protonation. Since the solvating capacities of these solvents are likely to be influenced by several factors like dielectric constant and hydrogen bond accepting or donating abilities, firm conclusions about solvent effects are premature at this stage.

Discussion

The results of this study establish that peptides **1** and **2** adopt backbone conformations that facilitate intramolecular interactions between the side chains of acidic and basic amino acid residues. In Boc-Asp-Pro-Aib-Lys-NHMe (**2**), the NMR results favor the formation of an intramolecular salt bridge between the aspartyl carboxyl group and the lysyl amino group. This structural feature appears to have considerable thermal stability in $(CD_3)_2SO$. Similar salt bridges involving Asp–Lys or Glu–Lys (residue $i \rightarrow$ residue $i \pm 3$ or $i \pm 4$) ion pair interactions have recently been postulated to stabilize the long central helix of troponin C (Sundaralingam et al., 1985). The considerable stability of the Asp–Lys salt bridge in **2** suggests that such interactions may enable the three turns in the troponin C helix to retain their helical nature even when they are fully exposed to the solvent. In the case of Boc-Asp-Pro-Aib-His-NHMe (**1**), the intramolecular salt bridge interaction displays a remarkable sensitivity to the nature of the solvent. Our results clearly suggest proton transfer from the aspartyl carboxyl group to the histidyl imidazole group in apolar solvents like chloroform, while such a process appears to be dramatically reduced in polar solvents like $(CD_3)_2SO$. Buried ionizable groups, if charged, could generate enormous electric fields in the low dielectric environment inside proteins. The existence of a buried Asp–His ion pair in the charge-relay system of serine proteases has been established from neutron diffraction studies (Kossiakoff, 1983). A survey of the environment of ionizable groups in 36 different globular proteins has revealed only seven completely buried salt bridges of which three are instances of Asp–His ion pair interactions, viz., Asp_{81}–His_{78} or –His_{69} and Asp_{122}–His_{69} in superoxide dismutase and Asp_{102}–His_{57} in a complex of trypsin with trypsin inhibitor (Rashin & Honig, 1984). These buried salt bridges can play not only a crucial structural role but also an important functional role in stabilizing charged transition states, when they occur in the catalytic sites of enzymes (Warshel et al., 1984). Studies of abnormal and chemically modified hemoglobins have shown that in 0.1 M NaCl about 40% of the alkaline Bohr effect of human hemoglobin is contributed by the C-terminal histidine-146β. In deoxyhemoglobin, the imidazole of this histidine forms a salt bridge with aspartate-94β; in oxyhemoglobin or (carbonmonoxy)hemoglobin, it accepts a hydrogen bond from its own NH group instead (Perutz et al., 1985). The altered pK values of this imidazole in the two states of hemoglobin make a significant contribution to the observed Bohr effect, whose interpretation in stereochemical terms by Perutz represents a milestone in our understanding of protein structure and function. It is well-known that the nature and delicate stereochemistry of amino acid residues that make up the catalytic sites of enzymes can directly influence their pH dependence. A beginning has been made toward tailoring the pH dependence of enzyme catalysis by the judicious substitution of a charged amino acid by its neutral counterpart (Thomas et al., 1985). Similar approaches of protein engineering are likely to yield the industrially useful thermostable enzymes of the future (Perutz, 1985).

The ability of intramolecular salt bridges to stabilize folded backbone conformations is demonstrated by a comparison of the temperature coefficients of backbone –NH– groups for peptides **1**–**3** (Table I). In peptide **2**, the intramolecularly hydrogen-bonded Lys $N^{\alpha}H$ and *NH*Me protons show extremely low $d\delta/dT$ values of 1.7×10^{-3} and 0.4×10^{-3} ppm/K, respectively. On the other hand, the *NH*Me protons in peptide **1** exhibit a significantly higher $d\delta/dT$ value of 1.9×10^{-3} ppm/K. Thus, temperature coefficient data clearly suggest the greater stability of the intramolecularly hydrogen-bonded conformation of peptide **2** (X = Lys) as compared to peptide **1** (X = His). A comparison of the $d\delta/dT$ values in the protected peptide **3** and deprotected peptide **1** provides yet another control to study the effect of side-chain electrostatic interactions of ionizable side chains on backbone flexibility. Interestingly, the His $N^{\alpha}H$ shows a $d\delta/dT$ value of 3.5×10^{-3} ppm/K for **3**, whereas this –NH– group in **1** has a $d\delta/dT$ value of 1.3×10^{-3} ppm/K, suggesting that side-chain electrostatic interactions in peptides may indeed confer additional stability to backbone hydrogen bonds. Backbone motions that distort intramolecular hydrogen bonds should result in higher $d\delta/dT$ values for specific NH groups. Salt bridges have been proposed to restrain the backbone flexibility and confer greater thermostability to proteins from thermophiles as compared to their mesophile counterparts (Perutz, 1978). Our data suggest that this may indeed be the case, since we have observed a direct correlation between the strength of side-chain salt bridge and the flexibility of backbone conformations. Thus peptide **3**, which is devoid of a salt bridge, shows the highest backbone NH $d\delta/dT$ values; peptide **1**, which has a salt bridge of intermediate strength, exhibits intermediate $d\delta/dT$ values for backbone NH protons, while peptide **2**, which has the strongest salt bridge, displays the lowest $d\delta/dT$ values for the shielded NH protons. The anomalously low $d\delta/dT$ value of the Aib NH group of peptide **2** may be a consequence of further nucleation of the 3_{10} helical conformation to generate a third type III β-turn, with Asp and Pro as the corner residues and having a 4→1 hydrogen bond, involving the Boc CO and Aib NH groups. There is considerable evidence in the literature for the occurrence of Pro at the amino termini of 3_{10} helical structures. For example, proline occurs at position 2 in the decapeptide Boc-Aib-Pro-Val-Aib-Val-Ala-Aib-Ala-Aib-Aib-OMe, which adopts an almost perfect 3_{10} helical conformation, both in the solid state (Francis et al., 1983) and in solution (Iqbal & Balaram, 1981). These peptides thus provide a good model for studying the role of salt bridges in the thermostability of proteins (Perutz, 1978).

The 270-MHz ^1H NMR spectra of the protected parent peptides Boc-Asp(OBzl)-Pro-Aib-His-NHMe and Boc-Asp(OBzl)-Pro-Aib-Lys(Z)-NHMe reveal the presence of additional resonances of low intensity (data not shown), suggesting that in solution minor conformations of these peptides coexist with the major conformations described. These arise presumably from the population of a cis conformation about the Asp–Pro bond. There is no evidence for the population of cis conformations in the deprotected peptides **1** and **2**, suggesting

that intramolecular electrostatic interactions between side-chain ionizable groups can influence backbone flexibility, by restricting geometrical isomerism about the peptide bond. The importance of such isomerizations in the folding of globular proteins has been recognized (Brandts et al., 1975).

It is interesting to note that pH-induced conformational transitions precede the penetration of proteins like diphtheria toxin into biomembranes. Here, salt bridges may act as sensors of surrounding pH (Blewitt et al., 1985). It has also been suggested that the pronounced conformational change from a protein structure characterized by a hydrophilic surface to one having a hydrophobic exterior may be mediated by cis–trans isomerizations about X–Pro peptide bonds (Deleers et al., 1983). The role of formation and disruption of salt bridges in influencing cis–trans isomerization along X–Pro peptide bonds of proteins in general and diphtheria toxin in particular remains to be investigated.

This study establishes that ion pair interactions between Boc-Asp-NHMe and Ac-Lys-NHMe or Boc-His-NHMe are much weaker than those in the intramolecular situations represented by peptides **1** and **2**. This was experimentally assessed by studying the effect of solvent polarity on imidazole protonation in the interactions between the side chains of Asp and His and by studying the effect of temperature on the interactions between the side chains of Asp and Lys. Minor increments in solvent polarity disrupted the process of proton transfer from Asp to His much more dramatically in the intermolecular case than in the intramolecular situation (Figure 8). Similarly, with increasing temperature Lys $C^{\epsilon}H_2$ resonances broadened rapidly in the Boc-Asp-NHMe + Ac-Lys-NHMe system, but increasing temperature had negligible effect on the chemical shift nonequivalence and multiplet structure of $C^{\epsilon}H_2$ proton resonances in **2** (data not shown). These observations are undoubtedly related to the fact that while intermolecular interactions are concentration-dependent, the intramolecular ones have no such dependence. The net effect is that the effective concentrations of interacting species in the intramolecular situation can vary between 0 and 10^{10} M (Creighton, 1983). "The low values occur when the two groups are held apart by the molecule to which they are attached; extremely high values occur when the two groups are held rigidly in optimal position for interaction even when they are not" (Creighton, 1983). This feature should be given due consideration in assessing the contribution of salt bridges toward the stability of globular proteins. In peptides **1** and **2**, stereochemical factors favor appropriate orientation of the charged groups for salt bridge formation, a feature that ensures a high "effective concentration" of the interacting species. It is interesting to note that when intermolecular interactions between two protein molecules are mediated via salt bridges as in the interaction of cytochrome *c* and cytochrome *c* peroxidase, the molecules seem to juxtapose several positively charged groups (lysines-13, -27, -72, -86, and -87 in cytochrome *c*) with negatively charged groups on their partners (aspartates-34, -37, -79, and -216 in cytochrome *c* peroxidase) (Salemme, 1976; Mathews, 1985). The marked clustering of positive charges on one protein and similar clustering of negative charges on the complementary protein seem to overcome the instability of intermolecular salt bridge interactions, presumably by a cooperative effect, which offsets the intrinsically unfavorable entropic nature of such interactions.

ACKNOWLEDGMENTS

We thank S. Raghothama for his help in the conduct of the NMR experiments, Dr. C. Toniolo, University of Padova, Italy, for the amino acid analyses, and Dr. M. Vijayan for a gift of *N*-acetyllysine *N'*-methylamide.

Registry No. **1**, 103884-55-5; **2**, 103884-56-6; **3**, 103884-57-7; HOBt, 2592-95-2; Asp, 56-84-8; His, 71-00-1; Lys, 56-87-1; Ac-Lys-NHMe, 6367-10-8; Boc-Asp-NHMe, 85127-42-0; Boc-His-NHMe, 103904-07-0; Boc-Pro-Aib-His-OMe, 103884-58-8; His-OMe·2HCl, 7389-87-9; His-OMe, 1499-46-3; Boc-Pro-Aib-OH, 79118-34-6; Boc-Pro-Aib-His-NHMe, 103884-59-9; Pro-Aib-His-NHMe, 103884-60-2; Boc-Asp(OBzl), 7536-58-5; Boc-Pro-Aib-Lys(Z)-NHMe, 103884-61-3; Boc-Pro-Aib-Lys(Z)-OMe, 103884-62-4; Lys(Z)-OMe, 24498-31-5; Boc-Asp(OBzl)-Pro-Aib-Lys(Z)-NHMe, 103884-63-5; Pro-Aib-Lys(Z)-NHMe, 103884-64-6; methylamine, 74-89-5.

REFERENCES

Anwer, K. M., & Spatola, A. F. (1980) *Synthesis*, 929–932.
Balasubramanian, T. M., Kendrick, N. C. E., Taylor, M., Marshall, G. R., Hall, J. E., Vodyanoy, I., & Reusser, F. (1981) *J. Am. Chem. Soc. 103*, 6127–6132.
Blewitt, M. G., Chung, L. A., & London, E. (1985) *Biochemistry 24*, 5458–5464.
Brandts, J. F., Halvorson, H. R., & Brennan, M. (1975) *Biochemistry 14*, 4953–4963.
Busa, W. B., & Nuccitelli, R. (1984) *Am. J. Physiol. 15*, R409–R438.
Bystrov, V. F., Portnova, S. L., Tsetlin, V. I., Ivanov, V. T., & Ovchinnikov, Yu. A. (1969) *Tetrahedron 25*, 493–515.
Cameron, T. S., Hanson, A. W., & Taylor, A. (1982) *Cryst. Struct. Commun. 11*, 321–330.
Creighton, T. E. (1983) *Biopolymers 22*, 49–58.
Deleers, M., Beugnier, N., Falmagne, P., Cabiaux, V., & Ruysschaert, J. M. (1983) *FEBS Lett. 160*, 82–86.
Francis, A. K., Iqbal, M., Balaram, P., & Vijayan, M. (1983) *FEBS Lett. 155*, 230–232.
Gilson, M. K., Rashin, A., Fine, R., & Honig, B. (1985) *J. Mol. Biol. 183*, 503–516.
Honig, B., & Hubbell, W. (1984) *Proc. Natl. Acad. Sci. U.S.A. 81*, 5412–5416.
Honig, B., Ebrey, T., Callender, R. H., Dinur, U., & Ottolenghi, M. (1979) *Proc. Natl. Acad. Sci. U.S.A. 76*, 2503–2507.
Hruby, V. J. (1974) *Chem. Biochem. Amino Acids, Pept., Proteins 3*, 1–188.
Iqbal, M., & Balaram, P. (1981) *J. Am. Chem. Soc. 103*, 5548–5552.
IUPAC–IUB Commission on Biochemical Nomenclature (1984) *Eur. J. Biochem. 138*, 9–37.
Kossiakoff, A. A. (1983) *Annu. Rev. Biophys. Bioeng. 12*, 159–182.
Markley, J. L. (1975) *Acc. Chem. Res. 8*, 70–80.
Mathews, F. S. (1985) *Prog. Biophys. Mol. Biol. 45*, 1–56.
Matthew, J. B. (1985) *Annu. Rev. Biophys. Biophys. Chem. 14*, 387–417.
Mayer, R., & Lancelot, G. (1981) *J. Am. Chem. Soc. 103*, 4738–4742.
Mitchell, P. (1961) *Nature (London) 191*, 144–148.
Nagaraj, R., & Balaram, P. (1981a) *Biochemistry 20*, 2828–2835.
Nagaraj, R., & Balaram, P. (1981b) *Acc. Chem. Res. 14*, 356–362.
Nakanishi, K., Balogh-Nair, V., Arnaboldi, M., Tsujimoto, K., & Honig, B. (1980) *J. Am. Chem. Soc. 102*, 7945–7947.
Perutz, M. F. (1978) *Science (Washington, D.C.) 201*, 1187–1191.
Perutz, M. F. (1985) *New Sci. No. 1460*, 12–15.
Perutz, M. F., Groneborn, A. M., Clore, G. M., Fogg, J. H., & Shih, D. T.-B. (1985) *J. Mol. Biol. 183*, 491–498.
Polgar, L., & Halasz, P. (1982) *Biochem. J. 207*, 1–10.

Prasad, B. V. V., & Balaram, P. (1983) In *Conformation in Biology* (Srinivasan, R., & Sarma, R. H., Eds.) pp 133–139, Adenine, New York.
Prasad, B. V. V., & Balaram, P. (1984) *CRC Crit. Rev. Biochem. 16*, 307–348.
Prasad, B. V. V., Balaram, H., & Balaram, P. (1982) *Biopolymers 21*, 1261–1273.
Rashin, A. A., & Honig, B. (1984) *J. Mol. Biol. 173*, 515–521.
Ravi, A., & Balaram, P. (1984) *Tetrahedron 40*, 2577–2583.
Ravi, A., Prasad, B. V. V., & Balaram, P. (1983) *J. Am. Chem. Soc. 105*, 105–109.
Roberts, G. C. K., & Jardetzky, O. (1970) *Adv. Protein Chem. 24*, 447–545.
Roos, A., & Boron, W. F. (1981) *Physiol. Rev. 61*, 296–436.
Salemme, F. R. (1976) *J. Mol. Biol. 102*, 563–568.
Smith, G. D., Pletnev, V. Z., Duax, W. L., Balasubramanian, T. M., Bosshard, H. E., Czerwinski, E. W., Kendrick, N. E., Mathews, F. S., & Marshall, G. R. (1981) *J. Am. Chem. Soc. 103*, 1493–1501.
Spray, D. C., & Bennett, M. V. L. (1985) *Annu. Rev. Physiol. 47*, 281–303.
Steitz, T. A., & Shulman, R. G. (1982) *Annu. Rev. Biophys. Bioeng. 11*, 419–444.
Stewart, J. M., & Young, J. D. (1969) *Solid Phase Peptide Synthesis*, Freeman, San Francisco.
Sundaralingam, M., Drendel, W., & Greaser, M. (1985) *Proc. Natl. Acad. Sci. U.S.A. 82*, 7944–7947.
Thomas, P. G., Russell, A. J., & Fersht, A. R. (1985) *Nature (London) 318*, 375–376.
Thornton, M. J. (1982) *Nature (London) 295*, 13–14.
Warshel, A. (1981) *Acc. Chem. Res. 14*, 284–290.
Warshel, A., Russel, S. T., & Churg, A. K. (1984) *Proc. Natl. Acad. Sci. U.S.A. 81*, 4785–4789.
Wold, F. (1981) *Annu. Rev. Biochem. 50*, 783–814.

Isolation and Characterization of a Lectin from the Cortical Granules of *Xenopus laevis* Eggs†

Tatsuro Nishihara,‡ Ron E. Wyrick,§ Peter K. Working,‖ Yee-Hsiung Chen,⊥ and Jerry L. Hedrick*
Department of Biochemistry and Biophysics, University of California, Davis, California 95616
Received December 20, 1985; Revised Manuscript Received June 9, 1986

ABSTRACT: A cortical granule lectin was isolated from eggs of the South African clawed toad *Xenopus laevis*. The lectin was released from the cortical granules by activation of dejellied eggs with the Ca^{2+} ionophore A23187. The lectin was purified by affinity chromatography with its natural ligand, the egg jelly coat, chemically coupled to a Sepharose matrix. The purified lectin was homogeneous by the criteria of isoelectric focusing (pI = 4.6), immunodiffusion, and immunoelectrophoresis but existed in two different molecular weight isomers as determined by sedimentation velocity ultracentrifugation and disc gel electrophoresis. Molecular weights of the isomers were determined by ultracentrifugation, disc gel electrophoresis, and gel filtration and found to be 539 000 and 655 000. Chemically, the lectin was a metalloglycoprotein, composed of 84.0% protein, 15.8% carbohydrate, and 0.19% calcium. No unusual types or amounts of amino acids were present. The carbohydrate moiety was composed of fucose, mannose, galactose, glucosamine, galactosamine, and sialic acid. The monosaccharide specificity of the lectin was investigated with the sugar inhibition of the precipitin reaction in gels. The lectin was specific for D-galactosyl sugars with the configuration at carbon atoms 2–4 of primary importance.

Fertilization in the eggs of the South African clawed toad *Xenopus laevis* results in marked changes in the morphology of the egg surface (Grey et al., 1974). In particular, the extracellular vitelline envelope, VE,[1] is converted to the morphologically distinct fertilization envelope, FE. The FE functions in blocking supernumerary sperm penetration at fertilization, the block to polyspermy reaction. It has been demonstrated that the isolated VE is readily penetrated by sperm whereas the isolated FE is impenetrable by sperm (Grey et al., 1976). Morphologically, the FE differs from the VE by the presence of a distinct ultrastructurally amorphous layer termed the fertilization (F) layer between the VE and the innermost jelly coat layer J_1 (Grey et al., 1974). Chemical and macromolecular analyses of the isolated envelopes, as well as microscopic evidence, indicated that the F layer is formed by interaction of components derived from the cortical granules and the innermost jelly coat layer, J_1 (Grey et al., 1974; Wolf et al., 1976).

We previously suggested that the interaction of the cortical granule and jelly components to form the F layer was, in molecular terms, a metal-mediated lectin–ligand interaction (Wyrick et al., 1974a,b; Nishihara et al., 1975). The purpose

† This work was supported in part by a grant from the USDHS, HD-4906.
‡ Present address: Laboratory of Microbiology, Suntory Institute for Biomedical Research, Mishima-Gun, Osaka, 618 Japan.
§ Present address: Director of Research, Hollister-Stier Laboratory, Spokane, WA 99220-3153.
‖ Present address: Chemical Industry Institute of Toxicology, Research Triangle Park, NC 27709.
⊥ Present address: Graduate Institute of Biochemical Sciences, National Taiwan University, Taipei, Taiwan, China.

[1] Abbreviations: ACFT, affinity column flow through; CG_{ex}, cortical granule exudate; CGL, cortical granule lectin; EDTA, ethylenediaminetetraacetic acid; EGTA, ethylene glycol bis(β-aminoethyl ether)-*N*,*N*,*N*′,*N*′-tetraacetic acid; FE, fertilization envelope; F layer, fertilization layer; J_1, jelly coat layer; NANA, *N*-acetylneuraminic acid; PAS, periodic acid–Schiff base; Tris-HCl, tris(hydroxymethyl)aminomethane hydrochloride; VE, vitelline envelope.

0006-2960/86/0425-6013$01.50/0